Appl. Phys. B (2017) 123:175
DOI 10.1007/s00340-017-6753-4

Applied Physics B
Lasers and Optics

A robust, alignment-free broadband CARS system based on stimulated processes in heavy water

Hong Yuan[1,2] · Baodong Gai[1,2] · Jinbo Liu[1] · Jingwei Guo[1] · Xianglong Cai[1] · Xusheng Xia[1,2] · Xueyang Li[1,2] · Baichao Zhang[1,2] · Liezheng Deng[1] · Yuqi Jin[1]

Received: 28 December 2016 / Accepted: 20 May 2017 / Published online: 25 May 2017

Abstract We have established a new method for realizing a typical "2-color" collinear CARS (coherent anti-Stokes Raman scattering) system. The system mainly consists of a laser source, a D_2O cell, and a spectrometer. The pump/probe beam and the Stokes beam are provided by SBS (stimulated Brillouin scattering) and BSRS (backward stimulated Raman scattering) of D_2O, respectively. The CARS system is statistically stable, and it is also a broadband and alignment-free system. Measurement of N_2 signal in air with this system is demonstrated. Detection of N_2 in 0.006 bar air is realized with this system. Time-resolved pulse shapes of SBS and BSRS are measured to confirm their generation. Transference of energy from the SBS pulse to the BSRS pulse is realized with a Rhodamine 101 dye cuvette and discussed. This results in a better energy distribution between the pump/probe and Stokes pulses for CARS.

1 Introduction

Since the discovery of coherent anti-Stokes Raman scattering by Maker and Terhune in 1965 [1], CARS has been an attractive non-intrusive in situ measurement technique for monitoring concentrations and temperatures of species [2, 3]. CARS is widely used in gas, liquid, and solid diagnostics and biological research for its high sensitivity and fluorescence-background-free property. A CARS process is a four-wave mixing process with the participation of a pump beam, a Stokes beam and a probe beam. The pump and probe beams can be the same beam; in such a case, the CARS system is a "2-color" system. An early design of the CARS system utilizes forward-generated SRS to act as a Stokes beam. The residual pump beam is used as the CARS pump/probe beam. These two naturally collinear beams are focused into the detection region and form an alignment-free CARS system [4]. However, in this configuration, the beam quality of the residual pump beam may be easily damaged by laser-induced plasma and thermal distortions, etc. [5]. With the development of the dye lasers and OPOs (optical parameter oscillators), Stokes beams have been realized by dye laser or OPO beams for their tunable wavelengths [6, 7]. Adjustments of the pump/probe beam and Stokes beam are required to satisfy the phase-match condition in the detection region.

Nevertheless, the idea to build an alignment-free CARS system is always attractive, especially in field circumstances such as combustion measurement, where complex shakes bring huge challenges for optical alignments. Several alignment-free CARS systems using different mechanisms have been proposed in recent years [8–10]. Currently, it is popular to develop a broadband Stokes source in a multi-species-detection CARS system. One of the methods is to use a femtosecond oscillator coupled with photonic crystal fiber (PCF) or tapered nonlinear fiber to generate a supercontinuum source (SC). For example, a SC between 1064 and 2200 nm has been obtained with an air-silica PCF [11], and a SC between 800 and 940 nm has been generated with a PCF-based SC-generation module [12]. Water has also been applied to generate a SC [13]. However, little research has been done on utilizing SBS and BSRS in a

✉ Jinbo Liu
liujinbo@dicp.ac.cn

[1] Key Laboratory of Chemical Lasers, Dalian Institute of Chemical Physics, Chinese Academy of Sciences, Dalian 116023, China

[2] University of Chinese Academy of Sciences, Beijing 100049, China

CARS system, which has the potential to be a main method of realizing an alignment-free broadband CARS system.

The stimulated processes, including SBS and SRS in water, have attracted much interest from researchers. They show different interactions, including promotion and suppression, from each other under different circumstances [14, 15]. The backward SBS beam has unique phase-conjugating properties [16, 17], which can be used to compensate phase distortions. The SRS in water is usually generated by the stretching vibrations of O–H bonds [18]. The SRS spectra can be influenced by the hydrogen-bond networks. There are efforts to develop high-efficiency SRS in water [19, 20].

In this work, a typical "2-color" collinear CARS system for measuring N_2 is realized using a single laser source, where the pump/probe and Stokes beams are provided by the SBS radiation and the BSRS radiation of D_2O. It is an alignment-free, easy-to-install, highly stable and low-cost collinear CARS system. N_2 is chosen as the testing object of our prototype in this CARS system because CARS spectroscopy has been extensively used to determine the temperature of flames by N_2 spectroscopy [21–24].

2 Experimental setup

A schematic diagram of the alignment-free CARS system is shown in Fig. 1. The laser source is a frequency-doubled Q-switched Nd:YAG laser (Powerlite-9020, Continuum; with output wavelength of 532 nm, repetition rate of 10 Hz and full width at half maximum (FWHM) of 10 ns). The 532-nm beam pumps D_2O to generate SBS at wavelength of 532 nm as the pump/probe beam and BSRS at wavelength of ~607 nm as the Stokes beam. D_2O is placed in a quartz cell (10-cm path length). A lens (L1, focal length $f = 50.8$ mm) focuses the 532-nm beam into D_2O. A beam isolator [a polarized beam-splitter cube (PBS) and a zero-order λ/4 wave plate at 532 nm (λ/4 WP)] isolates the SBS radiation and most BSRS radiation in the vertical direction of the 532-nm Nd:YAG laser, while the forward radiation is blocked by a beam dump. The SBS and BSRS radiations are purified by a 45° 500-nm short-pass dichroic mirror (DM). The DM can transmit blue radiation (anti-Stokes radiation generated from D_2O), which may overlap with the CARS signal in spectra. As an optional step, the SBS and BSRS radiations pass through a quartz dye cuvette (1-mm optical path length) containing Rhodamine 101 ethanol solution. The fluorescence spectrum of Rhodamine 101 is obtained by a spectrometer (HR4000, Ocean). In this work, dye can be used to amplify the BSRS beam by consuming the SBS beam to increase the Stokes/(pump or probe) intensity ratio, and the effect of this dye cuvette will be discussed in detail later. A lens (L2, focal length $f = 100$ mm) focuses the SBS and BSRS radiation into the detection region in air. Then, the generated CARS signal of N_2 is focused on the fiber end of the fiber-coupled spectrometer (FHR1000, HORIBA) by a lens (L3, focal length $f = 100$ mm). Three filters, namely, a 500-nm short-pass filter, a 550-nm short-pass filter and a 532-nm notch filter, are placed ahead of the fiber end to block the SBS and BSRS beams. All spectra in this work are given in wavenumbers (cm^{-1}).

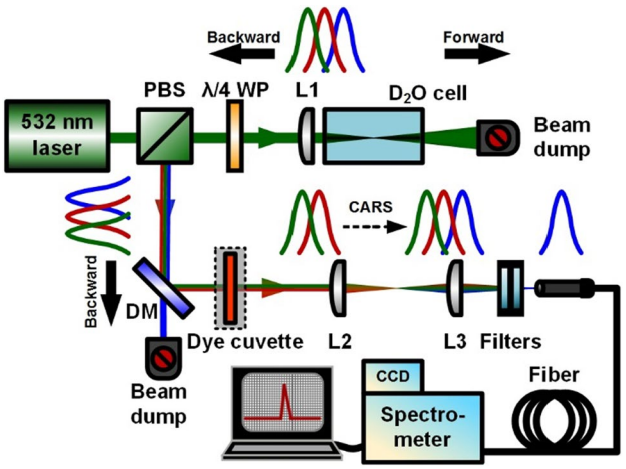

Fig. 1 Schematic illustration of the alignment-free CARS system. *PBS* polarized beam-splitter cube. λ/4 *WP* λ/4 wave plate at 532 nm. *L1* a convex lens with focal length $f = 50.8$ mm. *DM* 45° 500-nm short-pass dichroic mirror. *L2* and *L3* lenses with focal lengths $f = 100$ and 75 mm

3 Results and discussions

3.1 Spectral properties

In this CARS system, the BSRS of D_2O is utilized as a Stokes beam. The spectrum of the BSRS beam generated in D_2O is shown in Fig. 2 (obtained with FHR1000, HORIBA). The BSRS spectrum of D_2O shows a lower wavenumber wing, which ranges from its peak to ~2200 cm^{-1} at limited spectrometer sensitivity; the profile is in accordance with [25]. The enlarged local spectrum of 2200–2350 cm^{-1} is shown in the inset of Fig. 2. The input energy of the 532-nm beam into the D_2O cell is 45.4 mJ and the pulse energy of the BSRS is estimated to be close to 0.1 mJ. The energy-conversion efficiency of BSRS is close to 0.2%.

The SBS of D_2O is utilized as a pump/probe beam of this CARS system. It has a small frequency shift from the frequency-doubled Nd:YAG laser relative to the BSRS. The frequency shift is typically hundreds of GHz and cannot be discerned by the monochromator of the spectrometer. The pulse energy of the SBS beam is 9.5 mJ here, and the energy-conversion efficiency of SBS is 21%.

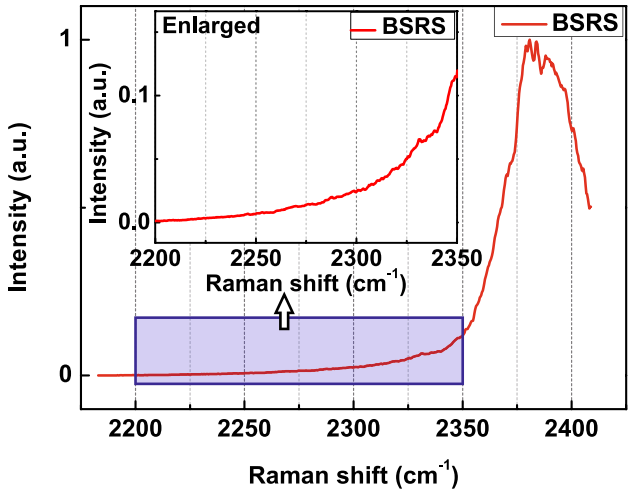

Fig. 2 BSRS spectrum of D_2O. The BSRS has observable intensity in a broadband range covering 2200–2400 cm^{-1}. *Inset* enlarged image of the area inside the *blue box*

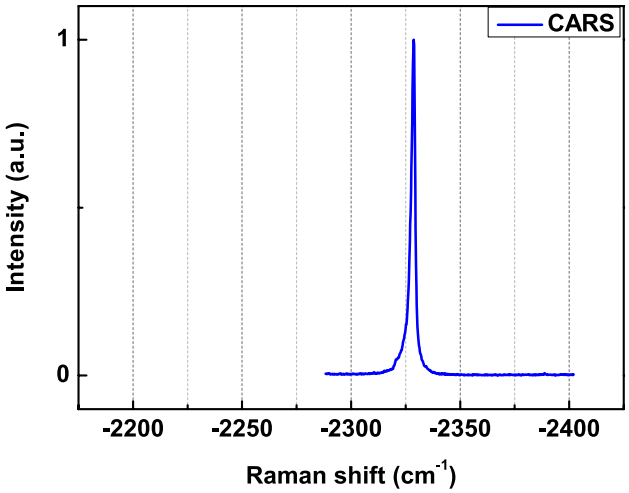

Fig. 3 N_2 CARS signal obtained using the SBS and BSRS of D_2O. The Raman shift is centered at 2329 cm^{-1}

The use of SBS and BSRS as pump/probe and Stokes beams of a CARS system has several advantages. It is well known that SBS and BSRS have the optical phase-conjugation property [16, 17]. The radiation re-emitted by a phase-conjugation mirror will compensate the phase distortion automatically, which will improve the beam quality [16, 26]. The pump/probe and Stokes beams are naturally collinear, so our CARS system can eliminate the requirement of frequently adjusting the light-path overlap between the pump/probe beam and the Stokes beam, which can be a frustrating task in traditional CARS systems.

D_2O is chosen in this demonstration for its low SBS threshold [27], similar Raman shift to N_2 and stable chemical properties: D_2O is inert, colorless, odorless, nontoxic, and nonflammable. Additionally, the products of its decomposition are deuterium and oxygen, which can escape from the liquid phase rapidly; so no decomposition product will affect the transparency of D_2O. In this work, no discernible transparency degradation of D_2O is observed over long-term use. Laser-induced filamentation and breakdown are fatal to solid optics components, such as laser crystals, nonlinear crystals and fibers, which can destroy the transparency of optics components. Conventional heat deposition of filamentation/breakdown results in melting and boiling of material [28]. However, although filamentation/breakdown may occur in D_2O, the damaged area can be substituted by surrounding molecules. Temperature changes may influence the generation efficiencies of SBS and SRS in water [20], and may also influence these processes in D_2O. The heat capacity of D_2O is large, so the temperature variation of D_2O can be quite small during use. In our experiment, the SRS generated from D_2O exhibits little change in efficiency and spectral distortion over time, which means the D_2O SRS profile can be kept statistically stable. Buzyalis et al. have used D_2O as the SBS scattering medium to form an SBS phase-conjunction mirror [27], through which SBS can compensate thermal distortions of the wavefront.

The BSRS peak of D_2O is wider [25] than the range from 2200 to 2400 cm^{-1}, and the Q-branch spectrum of high-temperature N_2 (from ~2265 to ~ 2352 cm^{-1}) is involved in it. Therefore, the CARS system can be used to detect N_2 in flame [24]. The SRS of D_2O has a broad Raman width, which is useful for multi-species detection as long as the detected species have Raman shifts that fall into the band of the D_2O BSRS spectrum. The SBS and BSRS are generated from D_2O almost synchronously [29] and collinearly. Air has a small refractive index and dispersion in the wavelength range of this work; so the phase-matching condition required by CARS is easily satisfied by a simple focusing optical path, using L2 in Fig. 1.

N_2 in air is successfully detected with the CARS system shown in Fig. 1 (obtained with FHR1000, HORIBA) without using a dye cuvette. Figure 3 shows the N_2 CARS signal. The N_2 CARS peak is centered at 2329 cm^{-1}, and its FWHM of 2 cm^{-1} is limited by the monochromator resolution. The discrepancy between the measured N_2 Raman shift (2329 cm^{-1}) and the reported value (2330.7 cm^{-1}) is quite small and can be explained by the monochromator error. To confirm that the CARS process occurs with the proposed system, a few comparative experiments are provided in this work. We replace the air with a mixture of argon gas and air in the detection region. The signal of N_2 decreases with the increase of the argon ratio. When a 550-nm short-pass filter is placed in front of the detection region to block the BSRS beam, the signal disappears. These results are consistent with a N_2 CARS process.

We also obtain the CARS signal under varying air pressure, as shown in Fig. 4 (obtained with FHR1000, HORIBA). The results are obtained without using the dye cuvette. A gas cell is used for controlling the gas pressure precisely. It is connected to a vacuum pump and a gas pressure gauge. The gas cell is a cylindrical stainless cell with optical windows at both ends. It is placed on the optical path of the detection region in this CARS system. The intensity of the CARS signal is proportional to the square of the air pressure in Fig. 4. Each data point in Fig. 4 is an average of 600 pulses. Linear fitting to the Intensity-(Pressure)^2 curve is carried out, giving (Intensity) = 0.93 (Pressure)^2, and the R^2 value of the fit is 0.988. The energy input 532 nm in front of the D_2O cell is 65.2 mJ and the pulse energy of the SBS is 15 mJ. N_2 in air at a pressure of 0.006 bar is successfully detected, and this is still above the detection limit. The results show that the CARS system has the potential for quantitative measurement.

3.2 Time-resolved pulse shapes

To obtain detailed information on CARS generation, pulse shapes of SBS and BSRS are measured. The output energy of the Nd:YAG laser is set to the same value as used in Figs. 2 and 3. SBS and BSRS radiations are separated using a grating and recorded simultaneously by two high-speed photodiodes whose bandwidth is broader than 1.2 GHz. The recorded temporal pulse shapes for SBS and BSRS radiations are displayed on a 20 GSa/s oscilloscope.

Pulse shapes of SBS and BSRS radiations, averaged over 200 pulses, are shown in Fig. 5. The instantaneous intensities of SBS and BSRS begin to rise at the same time, but BSRS reaches its peak faster than SBS. Figure 5 shows that the SBS and BSRS pulses arrive at the detection region at the overlapping time. This satisfies the condition of a CARS process.

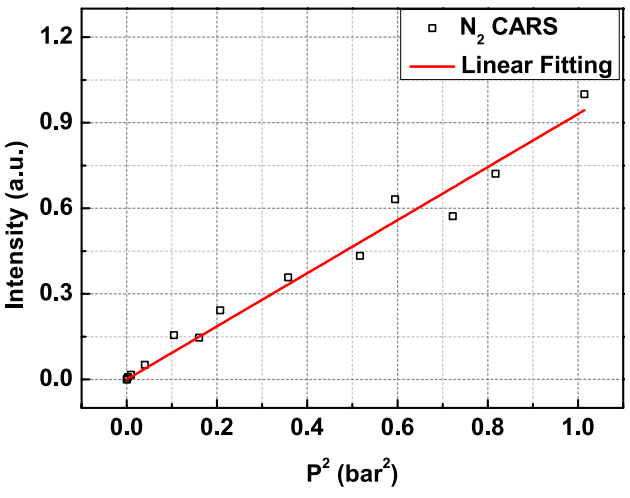

Fig. 4 CARS signal under different air pressures. It is plotted as the CARS intensity versus the square of the pressure (P), and linear fitting is carried out

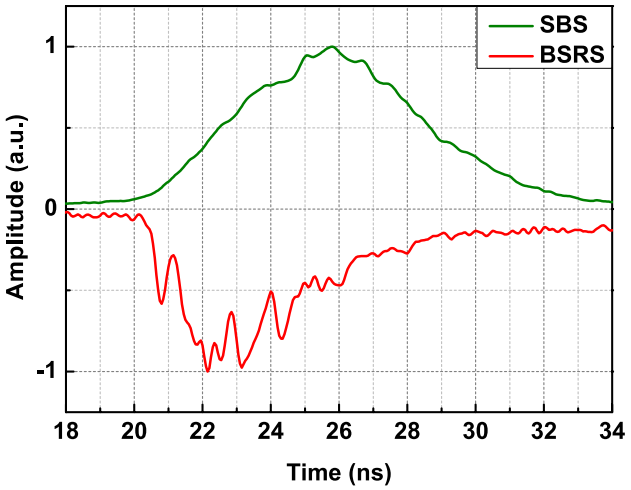

Fig. 5 Averaged pulse shapes of the SBS and BSRS radiations

Single-pulse sample shapes of SBS and BSRS radiations are shown in Fig. 6. It is observed that the single-pulse peak duration of BSRS radiations (FWHM ~300 ps) is much shorter than that of the 532-nm Nd:YAG laser, which indicates a pulse-compression effect. The BSRS peaks overlap with the corresponding SBS peaks in the time domain in Fig. 6, so it can be inferred that SBS is beneficial for the generation of BSRS. This is in accordance with several works on H_2O [15]. The pulse-compression effect is common in SRS. For instance, a 30-ps BSRS pulse has been formed from CS_2 pumped by a 15-ns laser in Maier's research [30]. A 2–3-ps BSRS pulse has been formed from CCl_4 pumped by a 27-ps laser in Arrivo's research [31]. An 80-ps forward SRS has been formed from H_2O pumped by

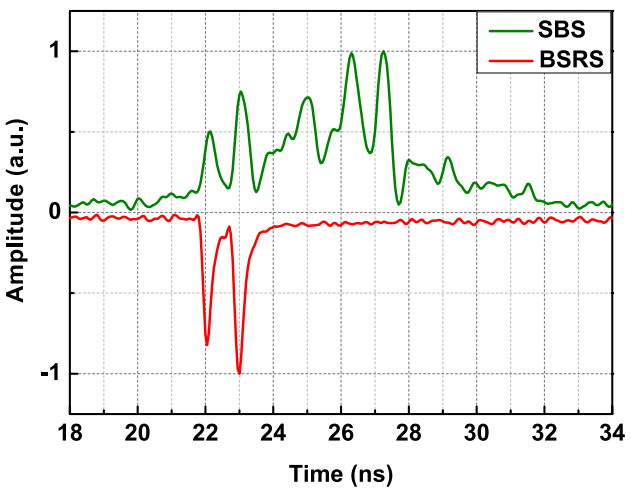

Fig. 6 Single-pulse shapes of the SBS and BSRS radiations

a 12-ns laser [32]. Though the BSRS energy is less than 0.1 mJ/pulse in this work, its narrow pulse width ensures a sufficient power density for CARS measurements in Fig. 3. The narrow BSRS peaks appear more frequently in the initial period of the SBS pulse in repeated measurements, as shown in Fig. 6. This trend is implied by the averaged curves in Fig. 5. Generally, BSRS and SBS can only be stimulated in the limited area near the focal point of L1, which is illustrated in Fig. 1. This phenomenon suggests that some kinds of accumulating variation of D_2O occur at the focal point of L1 in each pulse. This accumulating variation elevates the power requirements for generating BSRS. LIB occurs at the focal point of L1 in D_2O and broadband fluorescence can be observed. This broadband fluorescence comes from plasma formed in D_2O. The plasma accumulation over the period of one pulse should be the reason for the elevation of the power requirement for BSRS. Meanwhile, the threshold for the generation of SBS should be lower than for the generation of BSRS, so the SBS pulse should be much wider than the BSRS pulse. Figures 5 and 6 show that the BSRS and SBS pulses overlap in their appearance, within the limited time resolution of the photodiodes. It would be interesting to determine whether the pulses still overlap at higher time resolution. The generation of the CARS signal is strong evidence that they do.

3.3 CARS energy distribution optimization

In the backward emissions of 532-nm ns-pulse pumped water, the SBS (tens of mJ) is much stronger than the BSRS (less than 0.1 mJ). This energy distribution is not optimal for a CARS measurement. The probe beam shares the same wavelength with the pump beam in this case. Thus, the CARS intensity is proportional to the Stokes beam intensity and the square of the pump/probe beam intensity based on the classical model of the CARS process [33], which can be expressed as follows:

$$I_{\mathrm{CARS}} \propto I_{\mathrm{p}}^2 I_{\mathrm{S}} P_{\mathrm{i}}^2. \quad (1)$$

Here, I_{p} and I_{S} are the intensities of the pump/probe and Stokes laser beams; P_{i} stands for the partial pressure of the species detected by CARS and its quadratic relation can be verified in Fig. 4. When the total energy ($I_{\mathrm{p}} + I_{\mathrm{S}}$) is high, typically tens of mJ per pulse, laser-induced breakdown (LIB) may occur in the detection region. Sparks can be noticed when LIB occurs. LIB is an avalanche ionization process induced by the strong electric field of a strong laser, and high-temperature plasma forms as a consequence. In a high-temperature plasma, there are broadened atom/ion emission lines, molecular/molecular ion emission bands and radical emission bands. Here, broadening effect is related to collision broadening, Doppler broadening and Stark broadening. These lines and bands can occur at wavelengths shorter than that of the laser that induced the LIB. Therefore, an LIB process can generate strong, broadband emission in the wavelength band where CARS signals exist, which complicates CARS detection by submerging the CARS signals. As a rough estimate, the possibility of LIB in the detection region is supposed to be positively correlated with the total energy of the SBS and BSRS pulses. When I_{p} and I_{S} are closer, lower ($I_{\mathrm{p}} + I_{\mathrm{S}}$) is needed to generate a certain CARS intensity.

Here, a dye cuvette is applied to adjust this energy distribution to a more balanced one. Rhodamine 101 is chosen because its fluorescence curve (pumped by a 532-nm laser) covers the BSRS spectral range of D_2O, so the BSRS can be expected to receive full optical gain in an excited dye solution. The dye fluorescence curve in Fig. 7 shows a wider range than the BSRS curve (obtained with HR4000, Ocean). The dye consumes the energy of the 532-nm SBS beam for population inversion. Then, the BSRS beam is amplified by the population inversion in the dye. The spectral curve of BSRS amplified by dye (DBSRS) shows no significant shift or distortion when compared with that of BSRS in Fig. 7. The intensities at ~2330.7 cm^{-1} (which is the Raman shift of N_2, whose intensity influences the CARS signal intensity) in the curves of BSRS and DBSRS are shown in Fig. 8a; that in the DBSRS curve is ~2 times that in the BSRS curve. The total pulse energy measured before the CARS detection region (including both the BSRS and the SBS) is reduced from 9.5 to 3.2 mJ after adding the dye.

The CARS signal intensity slightly increases with the addition of dye, as shown in Fig. 8b. According to Eq. (1),

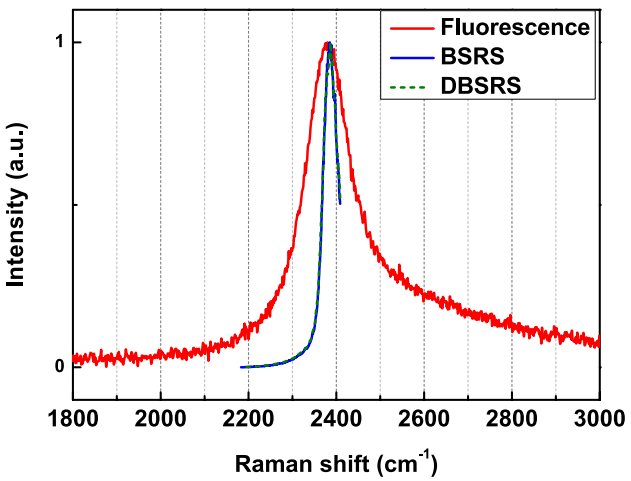

Fig. 7 Normalized dye fluorescence versus shift relative to a 532-nm Nd:YAG laser (Fluorescence); the normalized dye-amplified D_2O BSRS spectrum (DBSRS), and D_2O BSRS spectrum without amplification (BSRS) are given for comparison

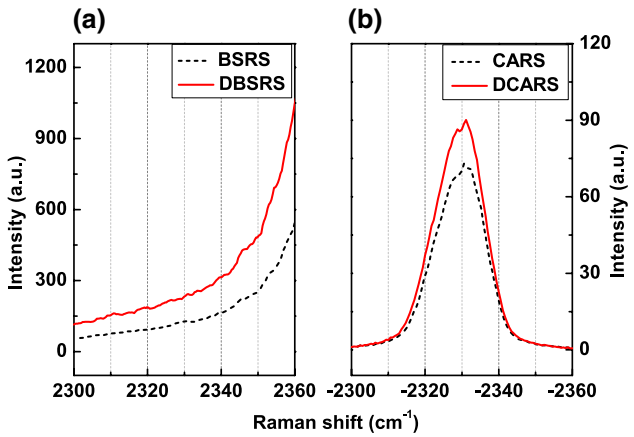

Fig. 8 Averaged spectra of local BSRS (**a**) and CARS (**b**) signals versus Raman shift. The *red solid lines* refer to the systems with dye (DCARS, DBSRS). The *black dashed lines* refer to the systems without dye. The large CARS linewidth is derived from a low spectrometer resolution setting

the large decrease of SBS intensity and the small increase of BSRS intensity should result in a weaker CARS signal; however, it seems that the CARS signal intensity is not in accordance with Eq. (1). At the same time, it is found that a dichroic-coated 532-nm beam attenuator (reflective type, inserted between DM and L2 in Fig. 1) can reduce the CARS intensity in accordance with Eq. (1). The dye solution produces saturable absorption and optical gain while a dichroic attenuator produces a fixed attenuation ratio, so we suppose that the pulse shapes of SBS and BSRS are changed by the addition of dye to form better overlap. Due to the limited photodiode time resolution, we have not yet discerned the fine change. Nevertheless, the reduction of the energy passing through the CARS detection region can reduce the risk of ionization, and the non-decreasing CARS signal intensity results in a more efficient detection when using Rhodamine 101.

This system still needs further optimization, especially to improve the BSRS intensity and the single-pulse stability. We can keep the temperature of D_2O stable using a temperature controller, or by adding fluorescent dye into the D_2O cell. According to Wang's research [34], the BSRS can be enhanced by the dye's fluorescence. In addition, splitting of the SBS and BSRS beams to test a sample gas cell and a reference gas cell simultaneously can be performed to calibrate the CARS measurement. A calibration device can also be developed by monitoring the SBS and BSRS intensities in real time. For example, a multi-channel spectrometer can be introduced to record the CARS and BSRS spectra simultaneously, and by using proper beam samplers, the pulse shapes of SBS and BSRS can be recorded without stopping the CARS process. Then, the CARS signal can be modified according to Eq. (1) to obtain better stability, towards the aim of single-pulse measurement of N_2.

4 Conclusion

We have demonstrated a new method for constructing a typical "2-color" collinear CARS system based on SBS and BSRS, which greatly simplifies the optical alignment. Due to the broad Raman shift and stable properties of D_2O, we can obtain a non-drifting broadband CARS system. The SBS and BSRS beams with high beam quality and high pulse power density, which are suitable for a CARS system, have been obtained. At the same time, we obtain the CARS signal under varying N_2 pressure, and the results reveal that the CARS system has the potential for quantitative measurement. The tests with this system indicate a detection limit of less than 0.006 bar (air pressure at which N_2 can be detected). The dye cuvette used in this system is helpful in reducing the possibility of LIB in detection. At last, we have given direct proof of simultaneous SBS and SRS production. The CARS system is an auto-aligned and broadband system and shows good stability over time. This system is a promising tool in liquid and solid species measurement. Moreover, it is possible to apply it to commercial spectroscopy, especially in some industrial conditions, for instance, in combustion detection. This auto-aligned CARS system is more robust, portable and low-cost compared with the traditional CARS system.

Acknowledgements This work is supported by National Natural Science Foundation of China (Grant Nos. 11304311, 11475177).

References

1. P.D. Maker, R.W. Terhune, Phys. Rev. **137**, A801–A818 (1965)
2. J. Bood, P.E. Bengtsson, M. Alden, Appl. Phys. B **70**, 607–620 (2000)
3. W. Clauss, V.I. Fabelinsky, D.N. Kozlov, V.V. Smirnov, O.M. Stelmakh, K.A. Vereschagin, Appl. Phys. B **70**, 127–131 (2000)
4. F.M.P.R. Regnier, J.P.E. Taran, AIAA J. **12**, 826–831 (1974)
5. H. Yui, T. Sawada, Phys. Rev. Lett. **85**, 3512–3515 (2000)
6. F. Beyrau, A. Datta, T. Seeger, A. Leipertz, J. Raman Spectrosc. **33**, 919–924 (2002)
7. G.W. Baxter, M.J. Johnson, J.G. Haub, B.J. Orr, Chem. Phys. Lett. **251**, 211–218 (1996)
8. H. Mikami, M. Shiozawa, M. Shirai, K. Watanabe, Opt. Express **23**, 2872–2878 (2015)
9. S. Kumar, T. Kamali, J.M. Levitte, O. Katz, B. Hermann, R. Werkmeister, B. Povazay, W. Drexler, A. Unterhuber, Y. Silberberg, Opt. Express **23**, 13082–13098 (2015)
10. H. Mikami, M. Shiozawa, M. Shirai, K. Watanabe, Opt. Express **23**, 17217–17222 (2015)
11. A. De Angelis, A. Labruyère, V. Couderc, P. Leproux, A. Tonello, H. Segawa, M. Okuno, H. Kano, D. Arnaud-Cormos, P. Lévèque, H.-O. Hamaguchi, Opt. Express **20**, 29705–29716 (2012)

12. J.G. Porquez, R.A. Cole, J.T. Tabarangao, A.D. Slepkov, Biomed. Opt. Express **7**, 4335 (2016)
13. J.A. Dharmadhikari, G. Steinmeyer, G. Gopakumar, D. Mathur, A.K. Dharmadhikari, Opt. Lett. **41**, 3475–3478 (2016)
14. D.M. Villeneuve, H.A. Baldis, J.E. Bernard, Phys. Rev. Lett. **59**, 1585–1588 (1987)
15. D.H. Liu, J.W. Shi, M. Ouyang, X.D. Chen, J. Liu, X.D. He, Phys. Rev. A **80**, 33808 (2009)
16. Zd Boris Ya, N.F. Pilipetskiĭ, V.V. Shkunov, Sov. Phys. Usp. **25**, 713 (1982)
17. B.Y. Zel'Dovich, N.F. Pilipetsky, VVe Shkunov, *Principles of phase conjugation* (Springer, Berlin, 2013)
18. H. Yui, H. Fujiwara, M. Fujinami, T. Sawada, Anal. Sci. **17**, i77–i79 (2002)
19. T. Slater, J.R. Tyrer, K. Williams, J. Mod. Opt. **48**, 1467–1477 (2001)
20. Y. Ganot, S. Shrenkel, B.D. Barmashenko, I. Bar, Appl. Phys. Lett. **105**, 061107 (2014)
21. P. Beaud, H.M. Frey, T. Lang, M. Motzkus, Chem. Phys. Lett. **344**, 407–412 (2001)
22. M. Scherman, M. Nafa, T. Schmid, A. Godard, A. Bresson, B. Attal-Tretout, P. Joubert, Opt. Lett. **41**, 488–491 (2016)
23. C.N. Dennis, C.D. Slabaugh, I.G. Boxx, W. Meier, R.P. Lucht, Proc. Combust. Inst. **35**, 3731–3738 (2015)
24. A.D. Cutler, L.M.L. Cantu, E.C.A. Gallo, R. Baurle, P.M. Danehy, R. Rockwell, C. Goyne, J. McDaniel, AIAA J. **53**, 2762–2770 (2015)
25. M. Sceats, S.A. Rice, J.E. Butler, J. Chem. Phys. **63**, 5390 (1975)
26. R.A. Fisher, *Optical phase conjugation* (Academic Press, New York, 1983)
27. R.R. Buzyalis, S.D. Aleksandr, E.K. Kosenko, Sov. J. Quantum Electron. **15**, 1335 (1985)
28. A. Couairon, A. Mysyrowicz, Phys. Rep. **441**, 47–189 (2007)
29. H. Yuan, B. Gai, J. Liu, J. Guo, H. Li, S. Hu, L. Deng, Y. Jin, F. Sang, Opt. Lett. **41**, 3335–3338 (2016)
30. M. Maier, W. Kaiser, J.A. Giordmaine, Phys. Rev. **177**, 580–599 (1969)
31. S.M. Arrivo, K.G. Spears, J. Sipior, Opt. Commun. **116**, 377–382 (1995)
32. H. Yui, Y. Yoneda, T. Kitamori, T. Sawada, Phys. Rev. Lett. **82**, 4110–4113 (1999)
33. J.W. Nibler, G.V. Knighten, *Coherent anti-stokes Raman spectroscopy. In Raman spectroscopy of gases and liquids* (Springer Berlin Heidelberg, Berlin, 1979), pp. 253–299
34. S. Wang, W. Fang, T. Li, F. Li, C. Sun, Z. Li, Z. Men, Opt. Express **24**, 10132–10141 (2016)